

Electronic Supplementary Information

Synthesis and PET imaging studies of [¹⁸F]2-fluoroquinolin-8-ol ([¹⁸F]CABS13) in transgenic mouse models of Alzheimer's disease

Neil Vasdev,^{*} Pengpeng Cao, Erik M. van Oosten Alan A. Wilson, Sylvain Houle,
Guiyang Hao, Xiankai Sun, Nikolai Slavine, Mustafa Alhasan, Peter P. Antich,
Frederick J. Bonte, and Padmakar V. Kulkarni

vasdev.neil@mgh.harvard.edu

General Information

All chemicals were obtained from commercial suppliers and were used as received without further purification unless indicated. All water used was distilled and deionized. Flash column chromatography purification was accomplished using silica gel 60 (63-200 μm , Caledon). Preparative thin layer chromatography (PTLC) was carried out using silica gel GF plates (20 cm \times 20 cm, 2000 μm) from Analtech.

A Scanditronix MC 17 cyclotron was used for radionuclide production. Purifications and analyses of radioactive mixtures were performed by HPLC with an in-line UV (254 nm) detector in series with a Bioscan radioactivity detector. Isolated radiochemical yields were determined with a dose calibrator (Capintec CRC- 712M).

Electrospray ionization mass spectrometry was conducted with MDS Sciex QStar mass spectrometer to obtain the high resolution mass spectra. Electron impact mass spectrometry was conducted on either a VG 70-250S or Waters GCT Premier mass spectrometer. One-dimensional proton, carbon-13 and fluorine-19 NMR spectra were recorded at 25 °C on a Varian Mercury 300 MHz or 400 MHz spectrometer with an autoswitchable H/F/C/P 5 mm probe with gradients. Proton NMR chemical shifts were reported using tetramethylsilane (TMS, 0.00 ppm) as an internal standard or referencing on residual CHCl_3 (at 7.26 ppm) or CH_3CN (at 1.94 ppm) and correcting to TMS. The ^{19}F NMR spectra were referenced relative to CFCl_3 . Yields were not optimized.

Synthesis of 8-(benzyloxy)-2-chloroquinoline (3)

8-Hydroxy-2-chloroquinoline, **2** (TimTec LLC; 1.0 g, 5.6 mmol), was dissolved in DMF (10 mL) in a round bottom flask. Potassium carbonate (1.6 g, 11.4 mmol) was added into

the flask followed by addition of benzyl chloride (1.3 mL, 11.4 mmol). The reaction mixture was stirred for 2 h at 60 °C. Completion of the reaction was monitored by thin layer chromatography (Hex/EtOAc/HOAc 89:9:2, v/v, $R_f = 0.3$ for **3**). Upon completion, the reaction mixture was extracted with CH_2Cl_2 (3×50 mL) and the combined organic fractions were extracted with H_2O (2×50 mL) and brine (50 mL). The organic layer was then dried (Na_2SO_4), filtered and concentrated to yield a light pink solid (1.33 g, 88.8%). Mp: 92 – 94 °C. ^1H NMR (CDCl_3 , 300 MHz) δ (ppm): 7.94 (d, $J = 8.6$ Hz, 1H, ArH), 7.41 (d, $J = 7.3$ Hz, 2H, ArH), 7.31-7.17 (m, 6H, ArH), 6.96 (dd, $J = 4.8$ Hz, $J = 2.0$ Hz, 1H, ArH), 5.34 (s, 2H, $-\text{CH}_2-$). HRMS (EI) calculated for $\text{C}_{16}\text{H}_{12}\text{ClNO}$ (+): 269.0607 amu, observed: 269.0607 amu. Isotopic pattern for Cl (3:1) was observed.

Synthesis of 8-(benzyloxy)-2-fluoroquinoline (**4**)

Compound **3** (50 mg, 371 μmol) and 6 mL of 1 M tetra-*n*-butylammonium fluoride (TBAF) in tetrahydrofuran (THF solvent was removed by rotary evaporation prior to usage) were added into DMSO (20 mL) in a septum-sealed 20 mL glass tube (Biotage). The reaction mixture was heated to 140 °C in a microwave reactor (Biotage Initiator) and stirred for 1 h. Reaction progress was monitored to completion by HPLC [Luna Phenyl-Hexyl 150 \times 4.6 mm; $\text{CH}_3\text{CN}/\text{H}_2\text{O}$ (65:35 v/v) + 0.1 N ammonium formate (AF); flow rate of 1 mL/min; monitored by UV ($\lambda = 254$)] until **3** ($t_R = 5.0$ min) was consumed. Completion of the reaction was further confirmed by thin layer chromatography (Hex/EtOAc/HOAc 89:9:2, v/v, $R_f = 0.5$). The reaction mixture was then diluted with 100 mL of H_2O and extracted with EtOAc (3×50 mL). The combined organic layer was dried (Na_2SO_4), filtered and concentrated. The residue was purified using PTLC

(Hex/EtOAc/HOAc 89:9:2, v/v) and eluted from the silica with MeOH/EtOAc (10:90, v/v), as described above, to yield an orange oil (17.9 mg, 38.2%). ^1H NMR (CD_3CN , 400 MHz) δ (ppm): 8.40 (dd, $J = 8.7$ Hz, $J = 8.7$ Hz, 1H, ArH), 7.58 – 7.39 (m, 7H, ArH), 7.31 (dd, $J = 7.5$ Hz, $J = 1.4$ Hz, 1H, ArH), 7.21 (dd, $J = 8.8$ Hz, $J = 3.2$ Hz, 1H, ArH), 5.31 (s, 2H, $-\text{CH}_2$). ^{19}F NMR (CD_3CN , 376 MHz) δ (ppm): -64.70 (dd, $J = 7.9$ Hz, $J = 2.2$ Hz). HRMS (EI) calculated for $\text{C}_{16}\text{H}_{12}\text{NOF}$: 253.0903 amu, observed: 253.0907 amu.

Synthesis of 2-fluoroquinolin-8-ol (1)

Compound **4** (35.8 mg, 0.141 mmol) was dissolved in anhydrous CH_3CN (5 mL) and transferred into a 10 mL glass V-vial with Teflon septum and screw cap. $\text{Pd}(\text{OH})_2$ (19 mg) and Pd/C (19 mg) were added into the vial followed by pressurization with a balloon filled with H_2 (g). The reaction mixture was stirred for 1 h at room temperature. It was then filtered and washed through diatomaceous earth (Celite 545). The filtrate was concentrated under reduced pressure to yield a dark brown viscous solid (12.9 mg, 55.9%). ^1H NMR (CD_3CN , 400 MHz) δ (ppm): 8.44 (dd, $J = 8.9$ Hz, $J = 7.9$ Hz, 1H, ArH), 7.68 (bs, 1H, $\Delta\nu_{1/2} = 4.6$ Hz, $-\text{OH}$), 7.50 -7.49 (m, 2H, ArH), 7.25– 7.21 (m, 2H, ArH). ^{19}F NMR (CD_3CN , 376 MHz) δ (ppm): -66.07 (d, $J = 6.2$ Hz). HRMS (ESI) calculated for $\text{C}_9\text{H}_7\text{FNO}$ (+): 164.0512 amu, observed $[\text{M}+\text{H}]$: 164.0506 amu.

Radiochemistry

Preparation of Reactive ^{18}F Fluoride. Fluorine-18-labeled fluoride was produced by the $^{18}\text{O}(\text{p},\text{n})^{18}\text{F}$ nuclear reaction, using a 17 MeV proton beam current to irradiate ^{18}O]H₂O (10-97% enriched, Medical Isotopes Inc.), which was subsequently removed

from the target and trapped on an anion exchange resin. The resin was eluted by backflushing with 1 mL of solution that contained potassium carbonate (9.8 mM) and 1:9 H₂O/MeOH (v/v) into an open glass test tube with 15 mg of 2,2,2-crypt (Kryptofix[®]) as previously described.¹ The test tube was placed in a 100 °C oil bath and the mixture was azeotropically dried with anhydrous CH₃CN (1.5 mL) under nitrogen flow. Compound **3** (3.0 mg, 0.011 mmol) dissolved in DMSO (0.25 mL) was transferred into the test tube with dry [K₂₂₂][¹⁸F]. The reaction mixture was briefly vortexed and placed in a 135 °C oil bath for 15 min. The test tube was removed from the heat and 5 mL of H₂O was added before being loaded onto a tC18 Sep-Pak (Waters; 15 pre-activated with 5 mL of CH₃CN and 5 mL of water). The Sep-Pak was rinsed with 5 mL of H₂O and eluted with anhydrous CH₃CN (1 mL) into a septum-sealed V-vial containing Pd(OH)₂ (8 mg) and Pd/C (8 mg). The reaction mixture was stirred at room temperature for 15 min under the pressure of a H₂ balloon. The reaction mixture was then diluted with 1 mL of warmed anhydrous CH₃CN (ca. 60 °C) and filtered through Celite. The filtrate was diluted with 3 mL of H₂O before loaded onto the reverse phase semi-preparative HPLC (Phenomenex Prodigy ODS Prep, 250x10 mm, λ = 254 nm) with a mobile phase consisting of CH₃CN/H₂O (30:70 v/v) + 0.1 N ammonium formate (AF) at a flow rate of 7 mL min⁻¹. The product, [¹⁸F]**1**, eluting at 13.5 min, was collected and analyzed by analytical HPLC (Figure S1, a and b). Analytical HPLC was performed using a Phenomenex Luna C18, 250 mm × 4.6 mm, 10 μm, and the sample was eluted with CH₃CN/H₂O (60:40 v/v) + 0.1 N AF using a flow rate of 1.1 mL min⁻¹. Authentic **1** co-eluted with the ¹⁸F labeled product under these conditions (*t*_R = 3.3 min; Figure S1, c) and under several different analytical HPLC conditions (mobile and stationary phases, pHs and wavelengths). The

product [^{18}F]**1** was isolated in $30 \pm 4\%$ ($n=5$) radiochemical yield (uncorrected for decay) in an overall time of 71 min, including formulation. The HPLC fraction containing [^{18}F]**1** was formulated by dilution (2 mL USP 8.4% sodium bicarbonate solution and 23 mL H_2O) followed by loading onto a t-C18 plus Sep-Pak[®] cartridge, (Waters; pre-activated with 10 mL EtOH followed by 10 mL H_2O). The C18 cartridge was then washed with 5 mL H_2O and eluted with 1 mL EtOH, followed by 10 mL saline into a glass dose vial, fitted with a rubber septum and vent needle, containing 1 mL 8.4% sodium bicarbonate solution. HPLC analysis of formulated [^{18}F]**1** revealed high radiochemical (>99%) and chemical purities of [^{18}F]**1**. The specific activity of the formulated product was 1248 mCi/ μmol , and the log D was 2.07 ± 0.03 for [^{18}F]**1**, as measured using our previously published method.²

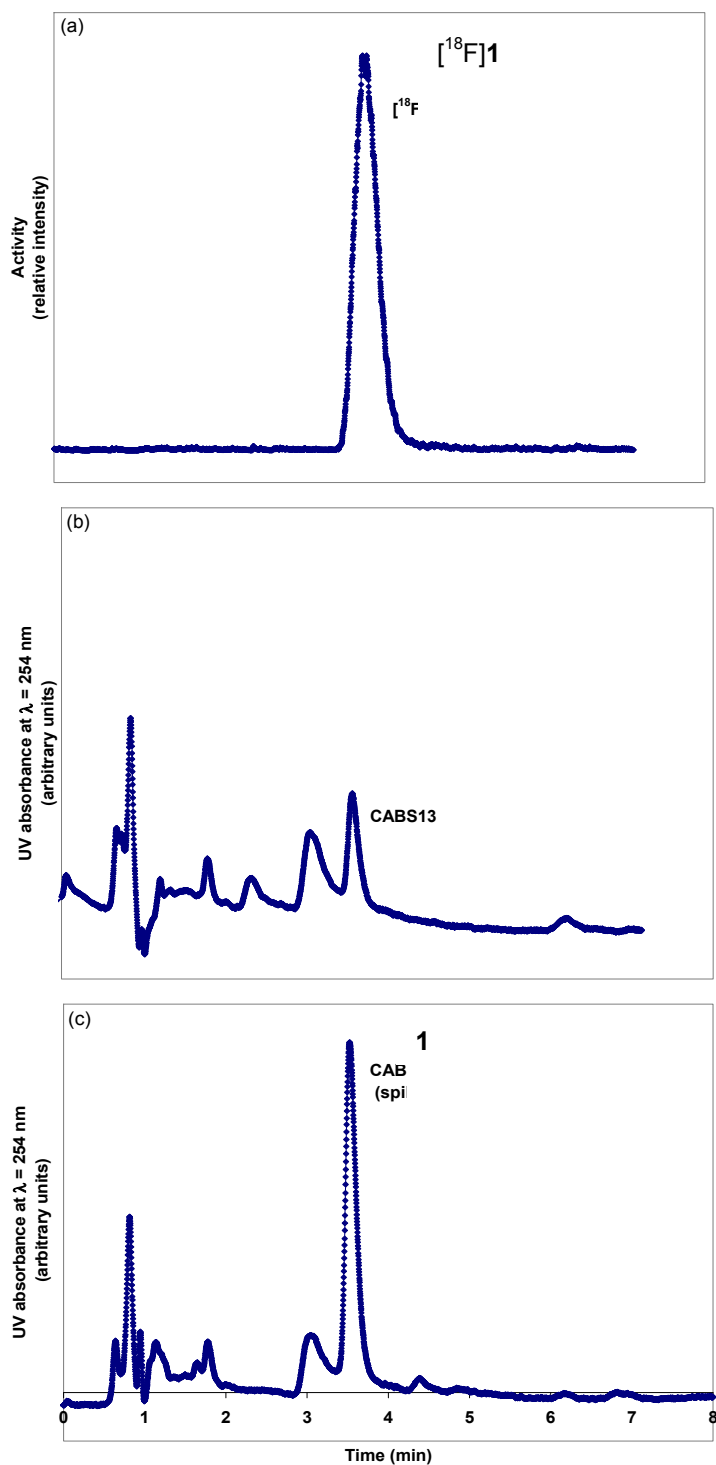


Figure S1. HPLC chromatograms ((a): radioactivity; (b); UV) of $[^{18}\text{F}]\mathbf{1}$ after purification.

The product co-injected with authentic $\mathbf{1}$ (c).

Synthesis of 4-bromoquinolin-8-ol

8-methoxy-4-bromoquinoline (1.0 g, 4.2 mmol) dissolved in CH₂Cl₂ (20 mL) was cooled to -40 °C using EtOH/dry ice. Boron tribromide solution (12.6 mL, 1.0 M in CH₂Cl₂) was added dropwise into the reaction mixture, which was then allowed to warm to room temperature for 24 h with stirring. Progress of the reaction was monitored by TLC (CHCl₃/EtOH 95:5, v/v, R_f of product = 0.8). Upon completion, the reaction mixture was treated with 12 mL of NaHCO₃, extracted with CH₂Cl₂ (3 × 60 mL) and EtOAc (1 × 25 mL). The combined organic layers were dried (Na₂SO₄), filtered and concentrated under reduced pressure to quantitatively yield a dark yellow solid (1.0 g, 100%). Mp: 128 – 130 °C. ¹H NMR (CDCl₃, 300 MHz) δ (ppm): 8.87 (d, *J* = 5.9 Hz, 1H, ArH), 8.47 (d, *J* = 5.9 Hz, 1H, ArH), 7.99 – 7.89 (m, 2H, ArH), 7.54 (dd, *J* = 7.5 Hz, *J* = 1.4 Hz, 1H, ArH), 4.92 (s, 1H, OH). LRMS (EI) calculated for C₉H₆BrNO (+): 223.0 amu, observed: 223.0 amu. Isotopic pattern for Br (1:1) was observed.

Synthesis of 8-(benzyloxy)-4-bromoquinoline

A solution of 4-bromoquinolin-8-ol (322 mg, 1.44 mmol) and benzyl bromide (350 μL, 2.9 mmol) in DMF (15 mL) was treated with K₂CO₃ (400 mg, 2.9 mmol) while stirring vigorously. The reaction mixture was heated to 60 °C and reacted for 48 h under N₂ balloon. Progress of the reaction was monitored by TLC (EtOAc/Hex/HOAc 9:89:2, v/v, R_f of product = 0.1). Excess benzyl bromide and DMF was removed by distillation at 60 °C, under vacuum. The resulting brown residue was dissolved in EtOAc (50 mL), washed with H₂O (3 × 25 mL) and brine (1 × 25 mL). The combined organic layers were dried (Na₂SO₄), filtered and concentrated to a white solid. The crude product was taken up with

EtOAc and purified by flash column chromatography and eluted with EtOAc/Hex/HOAc (9:89:2, v/v). Fractions containing the title compound were collected, combined and concentrated under reduced pressure to yield a yellow solid (238 mg, 52.7%). Mp: 121 – 123 °C. ¹H NMR (CDCl₃, 300 MHz) δ (ppm): 8.72(d, *J* = 4.6 Hz, 1H, ArH), 7.77-7.34 (m, 2H, ArH), 7.54 – 7.43 (m, 3H, ArH), 7.41 – 7.29 (m, 3H, ArH), 7.10 (dd, *J* = 7.8 Hz, *J* = 0.8, 1H, ArH), 5.45 (s, 2H, -CH₂-). LRMS (EI) calculated for C₁₆H₁₂BrNO: 313.0 amu, observed: 313.0 amu. Isotopic pattern for Br (1:1) was observed.

Synthesis of 8-(benzyloxy)-4-fluoroquinoline

8-(benzyloxy)-4-bromoquinoline (138 mg, 0.439 mmol) dissolved in 1.5 mL of Tetrakis[tris(dimethylamino)phosphoramylidenamino] phosphonium fluoride (P⁺F⁻) solution (0.4 mmol, 0.3 M in benzene) was added into a sealed 5 mL V-vial in a glove bag under argon and was stirred for 24 h at 120 °C. Completion of the reaction was monitored by TLC (MeOH/CH₂Cl₂ 2:98, v/v, R_f of product = 0.3). The crude product was diluted with 1 mL of CH₂Cl₂ and isolated via 3 PTLC plates and eluted with MeOH/CH₂Cl₂ (2:98, v/v). The product was isolated from the silica gel with 10% MeOH in CH₂Cl₂ and concentrated to an oil. The PTLC step was repeated with an additional plate to yield the title compound as a yellow solid (9.4 mg, 8.5%). The title compound was characterized by LRMS (EI) calculated 253.09, observed 253.0 and ¹⁹F NMR spectroscopy (CD₃CN, 376 MHz) δ (ppm): -64.5 ppm, however, this compound was unstable (decomposition observed in <24 h when stored under N₂ and at -20 °C) and was not further characterized or pursued.

Preliminary *In Vitro* Binding Assays:

A β peptide-Zn aggregates were prepared by incubating ZnCl₂ (25 μ M) in buffer PBS (pH 7.4) with A β peptide 1–42 (25 μ M) (Bachem Inc.) while stirring at room temperature for 1 hour. To ensure the aggregation of A β peptide, the mixture was incubated at 37 °C for 48 h. Binding studies were carried out in 12 mm \times 75 mm borosilicate glass tubes (9). A β -Zn aggregates (100 nM) were incubated with increasing concentrations of F-18 labeled HQ to a final volume of 1 mL for 30 minutes. All tubes were centrifuged for 10 minutes and the supernatant removed. The aggregates were washed again by adding 1 mL of PBS and centrifuging. Radioactivity in the aggregates was measured by a well type gamma counter (Perkin Elmer). Then the data were fitted into a binding-saturation equation using GraphPad Prism® software.

$$Y = B_{max} \times X^h / (K_d^h + X^h)$$

B_{max}: maximum binding, h: Hill slope, K_d: dissociation constant

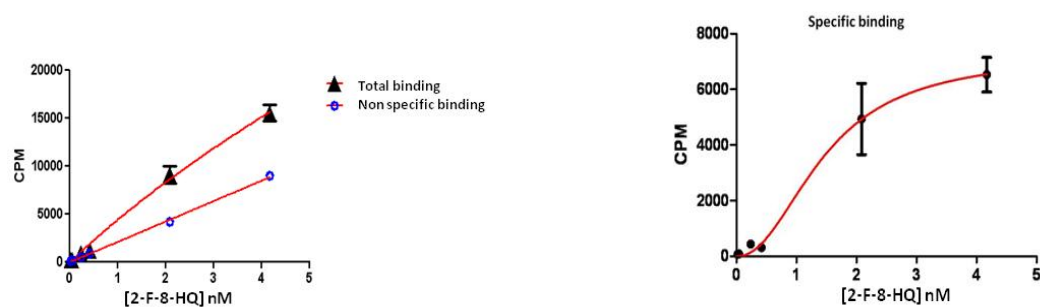


Figure S2. In vitro binding study. The first graph (left) shows the total and non specific binding. The second graph (right) shows the specific binding after subtraction of nonspecific binding and curve fitting. Data represent mean CPM (n=3) \pm SE.

The results showed high affinity to A β -Zn with a K_d value of 1.5 nM. The fitting showed that the Hill slope value is 2.2 which indicate that the receptor or ligand has multiple binding sites with positive cooperativity (Fig.S2). The K_d value is within the range reported (0.5-3.7nM) for previous amyloid plaques targeting agents.

Ex vivo autoradiography was correlated with immunohistopathological findings:

Autoradiography – Experimental Details:

Frozen brains sections of AD (12 months) and age matched control mice were cut in a cryostat at 10 μ m thicknesses. Brain sections were incubated with 200 μ L of [18 F]1 (50 μ Ci/ml) for 30 min. The slides were washed with PBS and air dried. The brain sections were exposed to Phosphor imaging plate for 2 hrs in the dark and images were quantified (PerkinElmer Cyclone® Storage Phosphor Imaging System). Image intensities were expressed as digital light unit (DLU/mm²) corrected for the background.

Immunohistochemistry

Experimental Details:

Following the autoradiography experiment, the same brain sections were stained with rabbit polyclonal anti-serum against A β -42 followed by Alexa488 labeled second antibody as described previously. Briefly, the brain sections were dried and fixed for 4h in paraformaldehyde and washed in PBS after incubation with A β -42 antibody and then with Alexa488 labeled second antibody. Finally, the sections were washed in PBS and viewed under a fluorescence microscope. Plaque density was quantified as previously described using Image J (NIH) software. Briefly, plaque regions were specified and both

area (pixels) and signal intensities were obtained. The plaque density was defined as the plaque area multiplied by the average plaque intensity.

Results and Discussion:

Autoradiography images (Fig. S3) showed higher uptake for AD brain sections in comparison to control (P=0.002). In addition, regional analysis for autoradiography demonstrated higher activity for the cortex and the cerebellum of AD mice brain sections in comparison to control mice brain sections (P=0.0018). Immunohistochemistry results showed variation in the plaques density (P=0.0149) in different regions of AD brain sections including cerebral cortex, hippocampus and the cerebellum while control mice showed negative results. It is interesting to note that AD mice cerebellar region had higher activity compared to control mice brain. Immunohistology showed the presence of plaques (though much lower in number compared to cortex region; Fig. S4).

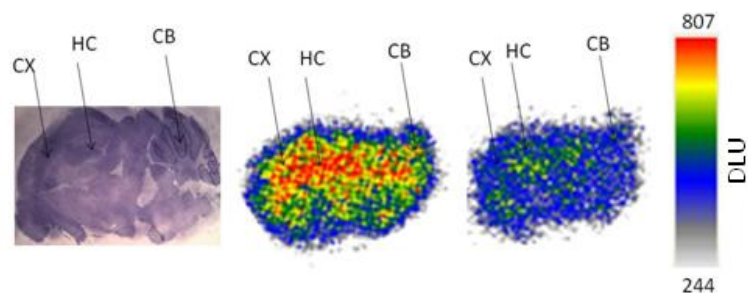


Figure S3. Brain section AD brain Control

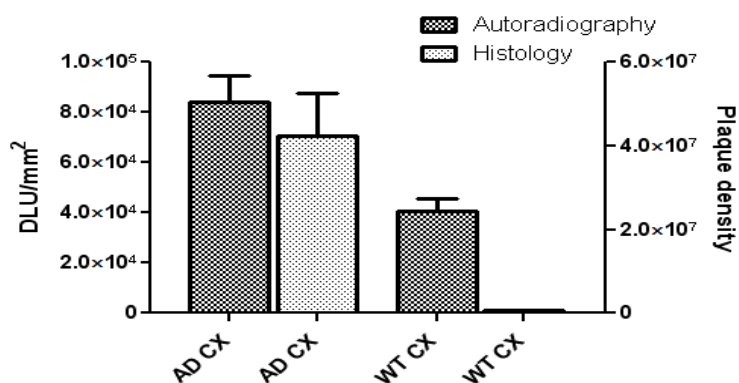


Figure S4 A. AD mice brain section (cortex) had high plaque density by histology and showed high light intensity whereas the control (wild type, WT) had no plaques and had much lower light intensity compared to AD mice brain sections ($p=0.03$). (CX=cortex).

Imaging studies in Transgenic mice

All animal experiments were carried out under humane conditions. Animal use protocols were approved by the Institutional Animal Care and Use Committee (IACUC) at UT Southwestern Medical Center at Dallas, TX.

Transgenic Mouse Models

Double transgenic mice with double mutation (APP/Ps1) for Alzheimer's disease were used (Strain: B6C3-Tg) (APP_{swe}, PSEN1dE9)85Dbo/J). This particular model correspond to a form of early onset of disease and expresses mutant human presenilin 1 (DeltaE9) and a chimeric mouse /human amyloid precursor protein (APP_{swe}). Tg mice were bred by the laboratory of Dr. Bao-Xi Qu (University of Texas, Southwestern) and characterized by genotyping. Control mice were of the same strain without gene transfection. Animals of both sexes were used. The weight of the animals was 35-45 grams. AD transgenic mice were somewhat sluggish in their movements; however one could not differentiate

between the two groups by general observation. Groups of mice (n=5) of ages 12-15 months were imaged in a Siemens Inveon® preclinical PET-CT imaging system.

Small Animal PET/CT Imaging

Experimental Details:

Small animal PET/CT imaging studies were performed using a Siemens Inveon® Multimodality PET/CT system (Siemens Medical Solutions Inc., Knoxville, TN, USA). Ten minutes prior to imaging, the animals were anesthetized using 3% Isoflurane at room temperature until stable vital signs were established. Once the animal was sedated, the animal was placed onto the imaging bed under 2% Isoflurane anesthesia for the duration of the imaging. The micro CT imaging was acquired at 80kV and 500 μ A with a focal spot of 58 μ m. The PET images were acquired directly following the acquisition of CT data. Radiotracer (50-90 μ Ci) was injected intravenously via the tail vein. Immediately following the injection, a 20-30 minute dynamic scan was performed. PET images were reconstructed using Fourier Rebinning and Ordered Subsets Expectation Maximization 3D algorithm with dynamic framing every 60 seconds.

Reconstructed images were fused and analyzed using Inveon® Research Workplace (IRW) software. For quantitation, regions of interest were placed in the areas expressing the highest radiotracer activity as determined by visual inspection. The resulting quantitative data were expressed in Percent Injected Dose per Gram (%ID/G). After imaging studies, animal brains were removed, fixed and brain tissue sections were stained with an antibody specific to A β and plaque burden measured with Image J NIH software.

Results and Discussion: PET images showed high (8-10 %ID/g) and fast (1 min) uptake in mice brains and rapid washout of the tracer from the control mice brains while Tg mice had delayed washout (Fig.S5 and S6; Table S1). Activity in the brain as a function of time was expressed as a sum of two exponential functions with different slopes: $f(t) = A1 * \exp(-B1*t) + A2 * \exp(-B2*t)$, where A1, A2, B1, B2 are fitting coefficients and were different (except for A1) for control (A1=104, A2=20.4, B1=1.32, B2=0.031) and AD (A1=104, A2=51, B1=1.46, B2=0.023) mice. Brain uptake ratio (Y) vs. time (X) was expressed by the equation $Y=1.36+0.36 * \ln(X)$ indicating persistent increase with time.

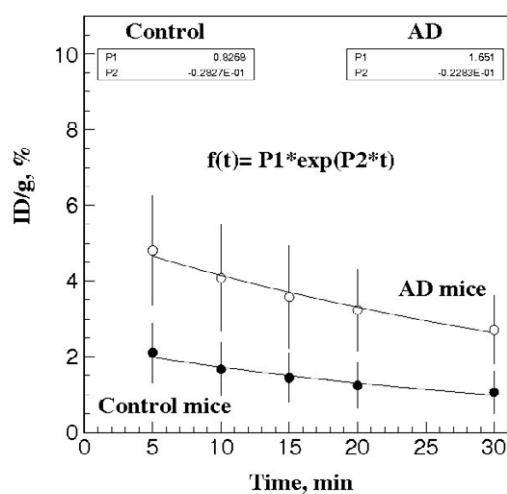


Figure S5. Time activity curves of AD and WT mice of the brain region.

Time (min)	%ID/g				
	5	10	15	20	30
AD (n=5)	4.81±1.45	4.08±1.42	3.58±1.36	3.23±1.07	2.71±0.91
WT (n=6)	2.10±0.86	1.66±0.76	1.44±0.70	1.24±0.66	1.06±0.61
P<0.05	0.012	0.011	0.009	0.007	0.005

Table S1. Summary of the %ID/g of AD and control mice and the statistical analysis at different time points.

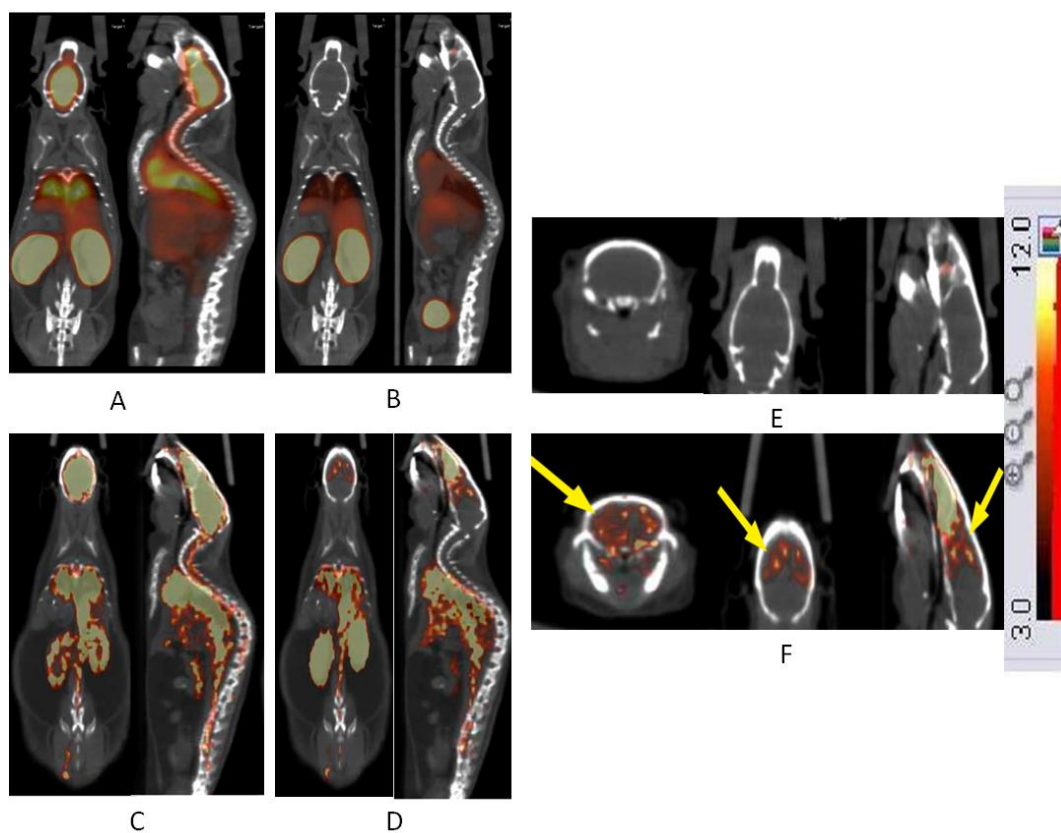


Figure S6. Control mice images at 0.5-1.5min post injection (A) and at 3.5-4.5min post injection. AD mice images at 0.5-1.5min post injection (C) and at 3.5-4.5min post injection (D). Control mice brain section in different views (E) in comparison to the AD mice (F). Units of the scale bar represent the %ID/g.

References

- 1 N. Vasdev, P. Seeman, A. Garcia, W. T. Stableford, J. N. Nobrega, S. Houle and A. A. Wilson, *Nucl. Med. Biol.*, 2007, **34**, 195-203.
- 2 A. A. Wilson, L. Jin, A. Garcia, J. N. DaSilva and S. Houle, *Appl. Radiat. Isot.*, 2001, **54**, 203-208.